

GEOREFERENCING OF MOMS-02 AND MISR STEREOIMAGES WITH STRICT SENSOR MODEL

Daniela Poli

Institute of Geodesy and Photogrammetry
Swiss Federal Institute of Technology, Zurich, Switzerland
daniela@geod.baug.ethz.ch

Commission I

KEY WORDS: Pushbroom, Georeferencing, Modeling, Orientation, Self-calibration, MOMS-02, MISR.

ABSTRACT

This paper presents a general sensor model for the georeferencing of imagery from CCD linear array sensors with along-track stereo viewing. The model is based on the classical collinearity equations extended and adapted to the specific characteristics of the acquisition of CCD linear scanners. It can be applied to single-lens and multi-lens sensors. In case of multi-lens optical systems, additional parameters are introduced in the basic single-lens model to describe the relative orientation of each lens with respect to the central one. As the sensor external orientation concerns, the position and attitude, which are different for each image line, are modeled with 2nd order piecewise polynomials depending on acquisition time, with constraints on the continuity of the functions and their first and second derivatives between adjacent segments. Additional pseudo-observations allow the modeling of the sensor position and attitude with 2nd or 1st order functions, according to the case study characteristics. A self-calibration has also been developed for the modeling of radial and decentering lens distortions, principal point(s) displacement, focal length(s) variation and CCD line(s) rotation in the focal plane.

Using well-distributed GCPs and, additionally, Tie Points (TPs), the external orientation and self-calibration parameters, together with the TPs ground coordinates, are estimated in a least-square adjustment. The calculations are performed in geocentric Cartesian system, geographic systems or local tangent systems.

In this paper the results obtained by applying the model on MOMS-02 and MISR (Multi Imaging SpectroRadiometer) are presented and discussed.

1. INTRODUCTION

In space applications CCD linear array sensors are widely used for acquisition of images at different ground resolution for photogrammetric mapping at different scales. The stereoscopy of the images is achieved across- or along- the flight direction. Sensors with across-track stereo capability are in most cases carried on spacecraft (SPOT1-4, IRS constellation) and combine one linear CCD array perpendicular to the flight direction with a rotating mirror. Sensors with along-track stereo capability scan the terrain surface in two different models. Multi-line CCD array sensors (MOMS-02, ASTER, SPORT5-HRS, MISR, WAOSS) consist of one or more lenses with CCD arrays placed parallel to each other, perpendicular to the flight direction and inclined with different viewing angles along the trajectory. The viewing angles are fixed and the strips (one for each CCD array) are acquired simultaneously. On the other hand single-line pushbroom sensors (IKONOS, EROS-A1) contain only one CCD array (or more segments placed closed to each other) and have the capability to rotate along the flight direction in order to re-scan the same area of interest. As result, they provide stereo images acquired from the same orbit from different directions. The main advantage of along-track stereo geometry with respect to the across-track one is that the time delay between the stereo images acquisition is smaller.

The images provided by linear CCD array sensors consist of lines scanned independently at different instants of time at different position and attitude. In most cases precise ephemeris provide the sensor position with high accuracy and instruments carried on board measure the rotation angles for some specific local reference frame on the satellite. Anyway an additional estimation of the correct external orientation is usually required. The sensor position and attitude are modelled with suitable

functions depending on time. Third order Lagrange polynomials (Ebner et al., 1992; Kornus, 1998) and quadratic functions (Kratky, 1989) have been proposed for this scope. In some cases, the sensor position at the time of interest is interpolated from the pass file provided by the space agency and only the attitude variations are modeled with linear functions (Westing, 1997).

In this paper the sensor model developed at our institute is described. A first version of the model was already presented in (Poli, 2002) and used for the georeferencing of MOMS-02 stereopairs. Then the model was improved with the integration of self-calibration and extended in order to be more flexible. The new results obtained from MOMS-02 georeferencing will be presented and discussed. The model has been also applied to other sensors carried both on airborne and satellite. The results obtained by the georeferencing of MISR images too will be shown.

2. SENSOR MODEL

The sensor model developed at IGP describes the relationship between image and ground coordinates, according to the geometry of the acquisition. In fact each image line is the result of a nearly parallel projection in the flight direction and a perspective projection in the CCD line direction. For each observed point, the relationship between image and ground coordinates is described by the collinearity equations. For sensors whose optical systems consist of more lenses, additional geometric parameters describing the relative position (Δx_j , Δy_j , Δz_j) and orientation (α_j , β_j , γ_j) of each lens j with respect to the nadir one are imported in the collinearity equations (Ebner, 1992).

Calling $[x, y]$ the point coordinates in the image system, f_j the focal length and $[x_j, y_j]$ the principal point position for lens j , the complete collinearity equations are described by:

$$\begin{aligned} x - x_{pj} &= -f_j \cdot \frac{N_x}{D} + \Delta x \\ y - y_{pj} &= -f_j \cdot \frac{N_y}{D} + \Delta y \end{aligned} \quad (1)$$

where N_x , N_y and D are expressions depending on the sensor external orientation, the ground coordinates of the (Ground Control Points) GCPs and Tie Points (TPs) and the relative orientation parameters between lenses.

Δx and Δy are the terms containing the self-calibration parameters. The aim of self-calibration is to model the systematic errors due to changes in the interior orientation, ns distortions and CCD line rotation in the focal plane. Δx and Δy contain the well-known additional parameters modeling the principal point displacement ($\Delta x_p, \Delta y_p$), the focal length variation (Δf), the symmetric (k_1, k_2) and decentering (p_1, p_2) lens distortion and the shear factor in y direction (s_y), as described in (Brown, 1971). Moreover the effect in x direction due to the CCD line rotation θ in the focal plane (Figure 1) is taken into account.

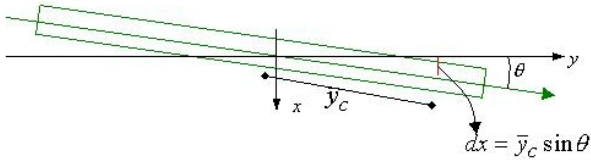


Figure 1. CCD rotation in the focal plane.

2.1 Trajectory modeling

The sensor external orientation is modelled by piecewise polynomial functions depending on time.

The platform trajectory is divided into segments according to the number and distribution of available GCPs and TPs. In each segment i the sensor external orientation ($X_C, Y_C, Z_C, \omega_C, \varphi_C, \kappa_C$) is modelled with second-order polynomials depending on the normalised time \bar{t} ($0 \leq \bar{t} \leq 1$):

$$\begin{aligned} X_C(\bar{t}) &= X_0^i + X_1^i \bar{t} + X_2^i \bar{t}^2 \\ Y_C(\bar{t}) &= Y_0^i + Y_1^i \bar{t} + Y_2^i \bar{t}^2 \\ Z_C(\bar{t}) &= Z_0^i + Z_1^i \bar{t} + Z_2^i \bar{t}^2 \\ \omega_C(\bar{t}) &= \omega_0^i + \omega_1^i \bar{t} + \omega_2^i \bar{t}^2 \\ \varphi_C(\bar{t}) &= \varphi_0^i + \varphi_1^i \bar{t} + \varphi_2^i \bar{t}^2 \\ \kappa_C(\bar{t}) &= \kappa_0^i + \kappa_1^i \bar{t} + \kappa_2^i \bar{t}^2 \end{aligned} \quad (2)$$

where $[X_0 X_1 X_2 \dots \kappa_0 \kappa_1 \kappa_2]^T$ are the parameters modeling the external orientation in segment i .

At the points of conjunction between adjacent segments, constraints on the zero, first and second order continuity are imposed on the trajectory functions: we force that the values of the functions and their first and second derivatives computed in two neighbouring segments are equal at the segments boundaries. As the point on the border between segment i and $i+1$ has $\bar{t}=1$ in segment i and $\bar{t}=0$ in segment $i+1$, applying the

zero order continuity for X_C function, we obtain:

$$\begin{aligned} X_C^i \Big|_{\bar{t}=1} &= X_C^{i+1} \Big|_{\bar{t}=0} \Rightarrow X_{instr} + X_0^i + X_1^i + X_2^i = X_{instr} + X_0^{i+1} \\ \frac{dX_C^i}{d\bar{t}} \Big|_{\bar{t}=1} &= \frac{dX_C^{i+1}}{d\bar{t}} \Big|_{\bar{t}=0} \Rightarrow X_1^i + 2X_2^i = X_1^{i+1} \\ \frac{d^2 X_C^i}{d\bar{t}^2} \Big|_{\bar{t}=1} &= \frac{d^2 X_C^{i+1}}{d\bar{t}^2} \Big|_{\bar{t}=0} \Rightarrow X_2^i = X_2^{i+1} \end{aligned} \quad (3)$$

In the same way, Equations (3) are written for $Y_C, Z_C, \omega_C, \varphi_C$ and κ_C functions and are treated as soft (weighted) constraints.

Additional pseudo-observations can fix some or all the 2nd order parameters to suitable values. An interesting application is that by fixing the 2nd order parameters to zero, the polynomial degree is reduced to 1 (linear functions). This option allows the modeling of the sensor position and attitude in each segment with 2nd or 1st order polynomials, according to the characteristics of the trajectory of the current case study.

2.2 Mathematical solution

The functions modeling the external orientation (Paragraph 2.1) are integrated into the collinearity equations (Equations 1), resulting in an indirect georeferencing model. Due to its non-linearity, the equations are linearized with the first-order Taylor decomposition with respect to the unknown parameters modeling the sensor external orientation (x_{EO}), the ground coordinates of the TPs (x_{TP}) and GCPs (x_{GCP}) and the self-calibration parameters (x_{SC}).

The initial approximations for the parameters modeling the sensor external orientation (x_{EO}^0) are calculated from the ephemeris or from the keplerian elements, according to the physical laws describing satellite orbit.

The initial values for the ground coordinates of the TPs (x_{TP}^0) are estimated with forward intersection, using the rough external orientation. The self-calibration parameters are approximated with null values.

Combining the observations equations and the constraints, the system:

$$\begin{cases} -e_{GCP} = A_{GCP} x_{EO} & + B_{GCP} x_{GCP} S_{GCP} x_{SC} - l_{GCP} \\ -e_{TP} = A_{TP} x_{EO} + B_{TP} x_{TP} & S_{TP} x_{SC} - l_{TP} \\ -e_{C0} = C_0 x_{EO} & - l_{C0} \\ -e_{C1} = C_1 x_{EO} & - l_{C1} \\ -e_{C2} = C_2 x_{EO} & - l_{C2} \\ -e_D = D x_{EO} & - l_D \\ -e_S = & S x_{SC} - l_S \\ -e_E = & + E x_{GCP} - l_E \end{cases} \quad (9)$$

is formed, where A_{GCP} and A_{TP} are design matrices for x_{EO} for GCPs and TPs observations; B_{GCP} and B_{TP} are the design matrices for x_{TP} for GCPs and TPs observations; C_0, C_1, C_2 are design matrices for constraints on zero, first and second order continuity; e and l are the discrepancy and observation vectors. All groups of observations are weighted according to the measurement accuracy.

The system is solved with least-squares method. In each iteration, the unknown vectors x_{EO}, x_{GCP}, x_{TP} and x_{SC} are estimated and added to the corresponding vectors used in the current iteration. The process stops when x_{EO}, x_{TP} and x_{SC} are

smaller than suitable thresholds. The number of GCPs and TPs depends on the overall number of unknowns, which varies according to the number of trajectory segments and the number of external orientation and self-calibration parameters that have been fixed.

The model requires few sensor characteristics: number of lenses, number of viewing directions, number of pixels in each line, focal length and principal point position of each lens, pixel size. All this data are easily accessible from the web or from literature, therefore any new sensor can be easily added.

In the next paragraph the tests applied on MOMS-02 will show the model capabilities.

3. GEOREFERENCING OF MOMS-02

A stereopair acquired by the German MOMS-02, mounted on the Russian MIR station, was used for our tests. The images were taken on March 14th, 1997, during the Priroda mission, from a height of approximately 400 km. MOMS-02 was a three-line sensor, with along-track stereo viewing provided by a high resolution nadir-looking lens (channel 5, 660 mm focal length) and two off-nadir lenses, looking forward (channel 6, +21.4 degrees, 237.25 mm focal length) and backward (channel 7, -21.4 degrees, 237.25 mm focal length) the MIR trajectory (Kornus, 1998).

The two images used in this work were taken over South Germany from channel 6 and channel 7, with a time delay of 40 seconds and a ground resolution of 18 m. The nadir image could not be used because channel 5 on Priroda was defocused. Each image has a dimension of 2976 pixels across-track and 5736 pixels along-track and consists of a combination of two overlapping scenes (scenes 25-26) in the flight direction. Approximations of MIR orbit (high precision ephemeris) and attitude (INS measurements) for the periods of acquisition of the two test scenes were kindly provided by DLR.

27 GCPs in regions free from clouds were acquired from a 1:50000 digital topographic map in Gauss-Krueger coordinate system; then they were manually measured in the left image and transferred to the other one with semi-automatic least-squares matching. Figure 3 shows the distribution of the 27 GCPs and the spacecraft trajectory.

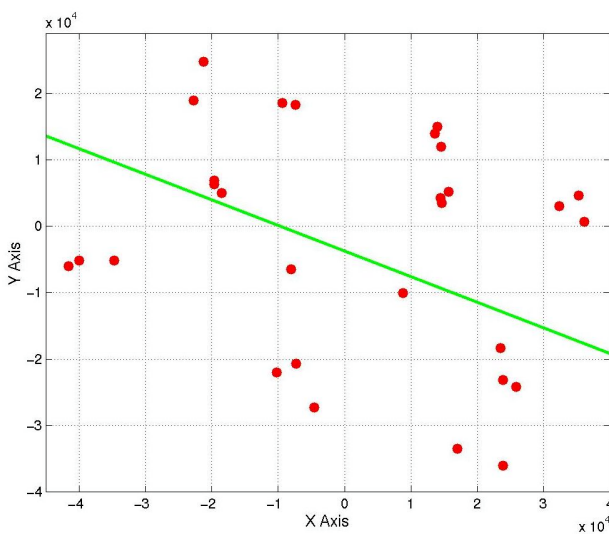


Figure 3. Spacecraft trajectory and distribution of GCPs in a local system.

3.1 Results

The general indirect georeferencing model was applied in order to orient the stereopair and estimate the ground coordinates of the TPs. The GCPs coordinates and the spacecraft were transformed into the geocentric Cartesian system. From the available 29 object points, a group of them was used as GCPs and the remaining as TPs. The estimated coordinates of the TPs were compared to the correct ones and used for the results' control. The tests were set as follows:

1. external orientation modeling with quadratic functions, varying the number of segments and GCPs, no self-calibration;
2. external orientation modeling with linear and quadratic functions, best GCPs configuration and best trajectory segments, no self-calibration;
3. self-calibration with best external orientation modeling configuration.

Test 1 was presented in (Poli, 2002). The results are here summarised in order to check the differences with the new results obtained after the model improvement. The spacecraft trajectory was divided into different number of segments (1, 2 and 4) and 6, 10 and 15 GCPs were used as ground information. The results are reported in Table 1. Taking into account the ground accuracy achieved and the minimum number of GCPs required, the best choice for the number of trajectory segments was 2. In this configuration RMS of 9.374 m in X , 7.136 m in Y and 12.347 m in Z (ground pixel size: 18 m) were obtained with 10 GCPs, corresponding to about 0.2, 0.4 and 0.7 times the pixel size.

From these first results, test 2 was performed in order to establish if the polynomial degree of the position or attitude functions could be reduced. Then the images were oriented using 10 GCPs, two segments configurations and linear functions for the attitude. The results in Table 2 show that the RMS improves, demonstrating that, at least with this particular dataset, 2nd order functions for both position and attitude produce better results. Therefore only one test was performed with linear functions for both position and attitude functions (Table 3). The large increase in the RMS of both TPs and CPs confirms the need of 2nd order functions for the external orientation modeling.

Finally a self-calibration was applied on the configuration with 10 GCPs, 2 trajectory segments and quadratic external orientation functions. The model allows the user to fix some self-calibration parameters and leave some others free, in order to estimate only the parameters of interest. Therefore the model was run different times fixing different self-calibration configurations. The RMS values of 17 CPs were used for the analysis. The self-calibration parameters that most effected the results were s_y (shear in CCD array direction) and dc (focal length variation). By fixing all parameters and keeping free only those two, RMS of 7.538m in X , 7.325m in Y and 9.175m in Z were obtained, corresponding to 0.42, 0.41 and 0.51 pixels respectively. The RMS achieved with the same configuration, but without self-calibration were 7.547m in X , 8.322m in Y and 8.786m in Z . From a comparison of the results, we see an improvement in X and Y coordinates, but 40cm increase in Z .

Anyways we observed that using self-calibration the system converges easier to the solution: the a-posteriori sigma of the full adjustment reduced considerably together with the RMS of GCPs.

GCP	TP	CP	RMS TPs (m)			RMS CPs (m)		
			X	Y	Z	X	Y	Z
2 segments								
6	0	21	-	-	-	11.588	11.082	9.715
6	21	0	15.996	11.594	20.685	-	-	-
10	0	17	-	-	-	7.547	8.322	8.657
10	6	11	8.711	7.510	10.076	7.101	8.983	8.786
10	17	0	7.831	7.133	11.600	-	-	-
4 segments								
10	0	17	-	-	-	6.957	6.500	9.113
10	6	11	7.864	7.380	10.548	6.346	5.899	9.361
10	17	0	7.327	6.675	11.119	-	-	-

Table 1. RMS for TPs and CPs using quadratic functions for position and attitude.

GCP	TP	CP	RMS TPs (m)			RMS CPs (m)		
			X	Y	Z	X	Y	Z
2 segments								
10	0	17	-	-	-	13.681	7.965	8.963
10	6	11	11.815	6.393	10.501	11.932	9.024	9.040
10	17	0	14.265	8.702	11.180	-	-	-
4 segments								
10	0	17	-	-	-	11.659	8.149	9.108
10	6	11	11.650	6.452	10.311	11.487	8.996	8.849
10	17	0	18.438	7.703	10.339	-	-	-

Table 2. RMS for TPs and CPs using quadratic functions for position and linear functions for attitude.

GCP	TP	CP	RMS TPs (m)			RMS CPs (m)		
			X	Y	Z	X	Y	Z
10	6	11	15.366	8.375	31.195	14.937	3.361	30.991

Table 3. RMS for TPs and CPs using linear functions for position and attitude (2 trajectory segments).

4. GEOREFERENCING OF MISR

The Multi-angle Imaging SpectroRadiometer (MISR) was successfully launched from NASA on 19 December 1999 on EOS-AM1 platform and has been continuously providing data since February 2000. MISR is a pushbroom scanner (Figure 2) that measures spectral radiances reflected in nine different directions and four spectral bands (446, 558, 672 and 866nm). The sensor consists of nine cameras labelled An, Af/Aa, Bf/Ba, Cf/Ca and Df/Da, acquiring stereo strips in nine different directions along the flight (0° , $\pm 26.1^\circ$, $\pm 45.6^\circ$, $\pm 60^\circ$ and $\pm 70.5^\circ$ respectively). The combination of instrument geometry and orbital characteristics (sun-synchronous, 705km altitude, near polar orbit) allows each point within a 360km-wide orbital swath to be observed from all nine directions within an interval of approximately 7 minutes. The ground footprint, which varies with the lenses and bands, remains constant in all cameras in the red band only (centred in 673nm) and is equal to 275m.

4.1 Data

Different kinds of operational data products from MISR are provided by NASA-JPL (Bothwell et al., 2002). In order to apply the sensor model and georeference the images, we used the level1B1 product, which is radiometrically but not geometrically corrected. From the granule corresponding to orbit 8836, path 195, acquired on 15th August 2001, only the strips corresponding to the central cameras Af, An and Aa were used. A segment over Europe was cut and pre-processed with

radiometric enhancement. From the four available bands, the red one only was used, because it maintains the same ground resolution in all cameras.

In order to find the initial approximation for the sensor position at the time of acquisition of each image line, the platform ephemerides for path 195 orbit 8826 were used. The time of acquisition of each image line was available from the metadata file. The ephemerides consisted of the sensor position and velocity at 2.5 sec time interval in ECI (Earth Centred Inertial) system, with X_{ECI} axis pointing to the vernal equinox, Z_{ECI} axis pointing to the celestial north pole and Y_{ECI} axis completing a right-hand coordinate system. The ephemerides were transformed into the fixed Cartesian geocentric system. Then the satellite position at the time of acquisition of each image line was calculated by interpolating the available measurements with cubic splines. Using the position rate of change available in metadata file the approximate values for the sensor attitude were also calculated.

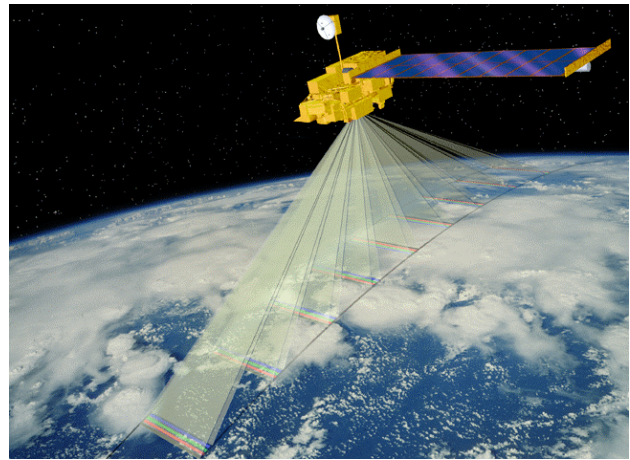


Figure 2. The Multi-imaging SpectroRadiometer [NASA website]. The sensor acquires nine strips simultaneously along nine different viewing directions

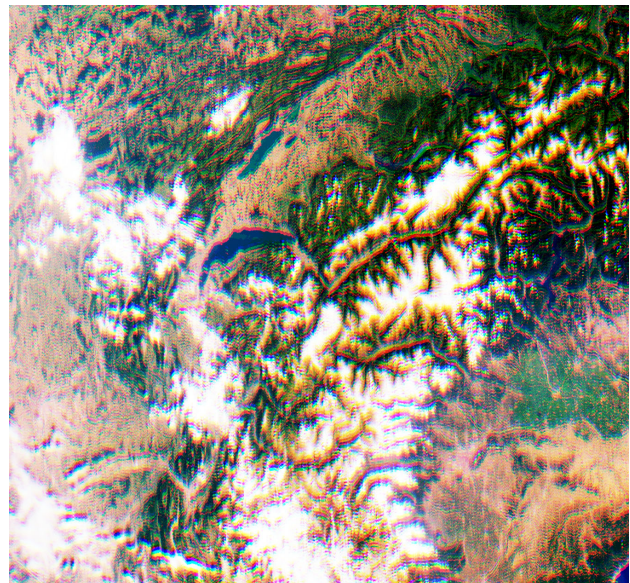


Figure 3. Zoom over Alps of combined RGB image.

4.2 GCPs identification

Due to the low image ground resolution, it was very difficult to search for GCPs. At first we compared the images and the cartographic maps of the corresponding areas in order to recognise some well-defined features, like rivers, seas and lakes borders (Figure 4), but this method was very time consuming and not very accurate.

The main problem was the identification of the features themselves in the images. For this reason we searched for points using other images of the same area with higher resolution. Requirements for the new images were a ground resolution smaller than 50m and low costs. The Landsat orthoproduct available in the Web for free was suitable for our tasks. This product consists of 30m resolution georeferenced images with planimetric coordinates in geographic (ϕ, λ) and UTM systems (E,N). 8 scenes from path 195 and 196 covering our area of interest were downloaded and pre-processed with radiometric enhancement. Then 3 level pyramid images (reduce factor of 2) were generated, so that the lowest level resolution (240m) was in the same range of the MISR scenes resolution (275m).

Common points were identified in Landsat 3rd level pyramid images and in Af, An and Af MISR images and matched with multi-photo least square matching (Figure 5). The image coordinates of the points of interest in Landsat images were transformed from the 3rd level to the original one and the corresponding geographic coordinates (ϕ, λ) were read in the Landsat original orthoimages. Using 1:25000 and 1:50000 scale topographic maps of the areas of interest the height coordinate was obtained. The ground coordinates of the matched points were transformed into Cartesian geocentric system.

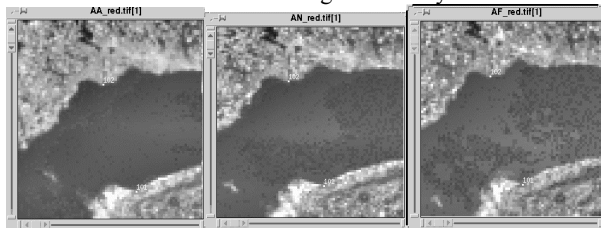


Figure 4. GCPs search in Aa (left), An (centre) and Af (right) images along Lake.

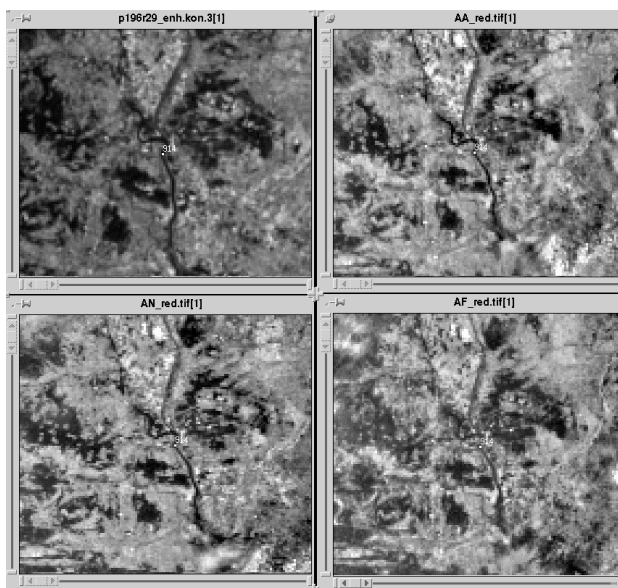


Figure 5. Point identification in Landsat 3rd level pyramid image (top-left), Aa (top-right), An (bottom-left) and Af (bottom-left) MISR cameras.

Two groups of GCPs were identified: one in North Germany and one in South France.

4.3 First results

The sensor model was applied on two distinct regions covered in the images, one over North Germany and one over South France, because in this areas a sufficient number of GCPs was measured.

For each region 6 ground points were available and were used all as GCPs. In both cases images acquired in the red band from Af, An and Aa cameras were used.

The model was applied in order to georeference the images. According to the tests performed on MOMS, the sensor external orientation was modeled with quadratic functions; due to the lack of information on the internal orientation, the self-calibration parameters were estimated too.

Tables 2 and 3 show the RMS for the GCPs in meters and pixels (ground pixel size: 275m). The accuracy of GCPs only are presented, because no other points were available as CPs.

As future task, new points will be measured in the same method above described and will be used as CPs.

	GCPs	RMS (m)		
		X	Y	Z
France	6	43.790	44.855	152.08
Germany	6	173.237	87.322	80.913

Table 2. Results (in m) of MISR georeferencing in France and Germany.

	GCPs	RMS (pixels)		
		X	Y	Z
France	6	0.16	0.16	0.55
Germany	6	0.63	0.32	0.29

Table 3. Results (in pixels) of MISR georeferencing in France and Germany.

The first results are satisfying, because the images have been oriented with sub-pixel accuracy.

The self-calibration was fundamental because it allowed the estimation of the correct internal and external orientation parameters. In the French and German tests, significant values for the principal point displacement have been estimated.

Without self-calibration, the RMS in GCPs were bigger than one pixel.

5. CONCLUSIONS

A general sensor model for multi-line CCD array sensors with along stereo viewing has been presented. The model combines the classic photogrammetric collinearity equations with the sensor external and internal orientation modeling, resulting in an integrated triangulation. The advantage of the proposed model is that it is flexible and can be applied imagery acquired by different sensors carried on satellite and on aircraft. When a new sensor is used, a small knowledge of its characteristics (focal length, pixel size, CCD array dimensions, viewing angles) is required.

In this paper the results obtained by the georeferencing of MOMS-02 and MISR pushbroom sensors have been presented. In particular tests have been performed on MOMS dataset in order to study the georeferencing accuracy achievable with different points distribution, different external orientation modeling functions and with/without self-calibration.

An accuracy of 0.2, 0.4 and 0.7 pixels in the CPs for X, Y and Z was achieved with the MOMS-02 stereo-pair, while for MISR

the accuracy for the GCPs only was available ().

From the results analysis, external orientation modeling with quadratic functions is recommended. Even if the estimated 2nd order parameters are small, they affect the ground accuracy.

As self-calibration concerns, it didn't produce any considerable improvements in MOMS results, but it was required in MISR case, where the knowledge of the internal orientation was poor.

As future work, the model will be improved and tested with other dataset. The tests on MISR will continue in order to get results from CPs and investigate the capabilities of the nine cameras for photogrammetric restitution.

ACKNOWLEDGEMENTS

This work is part of Cloudmap2 project, funded by the European Commission under the Fifth Framework program for Energy, Environment and Sustainable Development.

The EOS-Terra MISR data (level1B1 and ephemerides) were obtained from the NASA Langley Research Center Atmospheric Sciences Data Center.

REFERENCES

Bothwell, G.W., Hansen, E. G., Vargo, R. E., Miller, K. C., 2002. The Multi-angle Imaging SpectroRadiometer Science Data System, Its Products, Tools, and Performance. *IEEE Transactions of Geoscience and Remote Sensing*, Vol.40, No. 7, July 2002, pp. 1467-1476.

Ebner, H., Kornus, W., Ohlhof, T., 1992. A simulation study on point determination for the MOMS-02/D2 space project using an extended functional model. *International Archives of Photogrammetry and Remote Sensing*, Vol. 29, Part B4, Washington D.C., pp. 458-464.

Kornus, W., 1998. *Dreidimensionale Objektrekonstruktion mit digitalen Dreizeilenscannerdaten des Weltraumprojekts MOM-02/D2*. DLR-Forschungsbericht 97-54 (in German).

Kratky, V., 1989. Rigorous photogrammetric processing of SPOT images at CCM Canada. *ISPRS Journal of Photogrammetry and Remote Sensing*, No. 44, pp. 53-71.

Poli, D., 2002. General model for airborne and spaceborne linear array sensors. *International Archives of Photogrammetry and Remote Sensing*, Vol. 34, Part B1, Denver, pp.177-182.

Westin, T., 1990. Precise rectification of SPOT imagery. *Photogrammetric Engineering and Remote Sensing*, Vol. 56, No.2, February 1990, pp.247-253.